ATMOSPHERIC SCIENCE LETTERS
Atmos. Sci. Let. **18**: 238–245 (2017)
Published online 8 May 2017 in Wiley Online Library
(wileyonlinelibrary.com) **DOI:** 10.1002/asl.748

RMetS
Royal Meteorological Society

Assimilating GPM hydrometeor retrievals in HWRF: choice of observation operators

Ting-Chi Wu* and Milija Zupanski

Cooperative Institute for Research in the Atmosphere, Colorado State University, Fort Collins, CO, USA

**Correspondence to:*
T.-C. Wu, Cooperative Institute for Research in the Atmosphere, Colorado State University, 1375 Campus Delivery, Fort Collins, CO 80523, USA.
E-mail: ting-chi.wu@colostate.edu

Received: 6 December 2016
Revised: 2 March 2017
Accepted: 23 March 2017

Abstract

A recent study investigated the capability to assimilate hydrometeor retrievals in the National Oceanic and Atmospheric Administration (NOAA) Hurricane Weather Research and Forecasting (HWRF) system. Hydrometeor retrievals were obtained from a hurricane-specific retrieval that utilizes data from the Global Measurement Mission Microwave Imager. Data assimilation system used in HWRF is the hybrid ensemble-variational Gridpoint Statistical Interpolation (GSI). As a first attempt to assimilate hydrometeor retrievals in HWRF, observation operators for solid and liquid integrated water content were developed using the GSI standard control variables, such as temperature, pressure, and specific humidity, under the assumption that all water vapor in excess of saturation is condensed out. To improve the usefulness of assimilating hydrometeor retrievals in HWRF, this study extends this previous work by introducing new observation operators that (1) directly use hydrometeor species estimated from HWRF microphysics and (2) include total cloud condensate as a control variable. Hurricane Gonzalo (2014) was used to examine the performance of the old and new observation operators on HWRF analysis and subsequent forecasts with three pairs of experiments. Results suggest that when new observation operators are used the analysis is an improved fit to observations and realistic adjustments to control variables are evident as seen in analysis increment. In addition, the forecasts also indicate some improvements in hurricane intensity.

Keywords: **data assimilation; hydrometeor retrievals; HWRF; observation operators; cloud microphysics**

1. Introduction

Hurricane intensity and structure are fundamentally related to clouds. Among all the available observations, the use of all-sky satellite radiances and satellite-retrieved hydrometeors (e.g. Boukabara *et al.*, 2013; Kummerow *et al.*, 2015) are especially important for improving hurricane forecasting, because they contain valuable information about cloud and precipitation that often occur in sensitive regions in terms of forecast impact (Bauer *et al.*, 2011). While techniques to assimilate these observations (Bauer *et al.*, 2010; Zhu *et al.*, 2016) are currently used on a global scale (Global Forecast System; GFS), implementation on a regional scale is yet to be done. In this study, the National Oceanic and Atmospheric Administration (NOAA) operational Hurricane Weather Research and Forecasting (HWRF) system (Tallapragada *et al.*, 2015) is used as a representation of such regional scale model that currently assimilates neither all-sky satellite radiances nor hydrometeor retrievals.

As a preliminary attempt toward assimilating hydrometeor retrievals in HWRF, techniques were developed. In Wu *et al.* (2016), two observation operators to assimilate integrated solid–water content (SWC) and liquid–water content (LWC) are implemented in the hybrid Gridpoint Statistical Interpolation (GSI; Wu *et al.*, 2002; Kleist *et al.*, 2009; Wang, 2010). The integrated SWC and integrated LWC were obtained from a hurricane-specific microwave retrievals that utilizes data from the Global Measurement Mission (GPM) Microwave Imager (GMI), referred to as Hurricane Goddard PROFiling algorithm (GPROF) (Brown *et al.*, 2016). These two observation operators were built based on the assumption that super-saturated water vapor will condense out; the one for integrated SWC, referred to as $h_{\text{s\_noHydro}}$, is,

$$h_{\text{s\_noHydro}} = \sum_{k=k_0}^{k_{\max}} \left[\left(\frac{q^k}{1-q^k} \right) - 0.622 \frac{e_s\left(T^k\right)}{P^k - e_s\left(T^k\right)} \right] \cdot \frac{\Delta P^k}{g} \qquad (1)$$

and the one for integrated LWC, referred to $h_{\text{l\_noHydro}}$, is,

$$h_{\text{l\_noHydro}} = \sum_{k=1}^{k_{\text{mix}}} \left[\left(\frac{q^k}{1-q^k} \right) - 0.622 \frac{e_s\left(T^k\right)}{P^k - e_s\left(T^k\right)} \right] \cdot \frac{\Delta P^k}{g} \qquad (2)$$

where T is temperature, P is pressure, q is specific humidity, e_s is saturation vapor pressure, the superscript k denotes the model level index, k_0 is the vertical level where temperature is $T_0 = 273.15$ K, k_{mix} is the vertical level where temperature is $T_{\text{mix}} = 253.15$ K, $k_{\max}$ is the index for the top model level, ΔP^k is pressure difference between two vertical levels k and $k+1$ (i.e.

$\Delta P^k = P(k) - P(k+1)$), and g is the acceleration due to gravity.

Due to the super-saturation assumption that only depends on temperature, specific humidity, and temperature, there was no need to include cloud condensate as an additional control variable. However, as pointed out by Wu *et al.* (2016), using $h_{\text{s\_noHydro}}$ and $h_{\text{l\_noHydro}}$ may potentially create a negative bias of the guess due to the use of already saturated-then-condensed water vapor. Because of the potential negative bias and the lack of cloud condensate updates, new techniques have been developed that include new observation operators, which directly use cloud microphysical variables. This is done by including total cloud condensate mass (CWM) as control variable and adding individual hydrometeor species (cloud water, rain, ice, snow, graupel, and hail) as state variables; a technique that follows the GSI all-sky implementation developed by Zhu *et al.* (2016).

2. Methodology

2.1. Preparation of background hydrometeor species

The HWRF v3.7a release (Tallapragada *et al.*, 2015) is employed in this study. Among the various HWRF physics packages, cloud microphysics scheme is most directly related to the assimilation of hydrometeor retrievals because microphysics explicitly handles the behavior of hydrometeor species. The Ferrier–Aligo microphysics scheme (Aligo *et al.*, 2014) employed by HWRF predicts changes in water vapor mixing ratio (q_v) and CWM, which is the combined sum of individual hydrometeor species that include cloud water (q_l), rain (q_r), cloud ice (q_i), snow (q_s), graupel (q_g), and hail (q_h). Since individual hydrometeor species are not prognostic variables, they are diagnosed from CWM with the use of partition parameters that include fraction of ice (F_ICE), fraction of rain (F_RAIN), and values of riming rate (F_RIMEF).

2.2. CWM partition

There exist one formula in GSI that can be used to partition CWM into individual hydrometeor species (q_l, q_i, q_r, q_s, q_g, q_h) with the use of F_ICE, F_RAIN, and F_RIMEF. This formula, referred to as P6, is part of a routine called *cloud_efr_mod.f90*. This routine takes CWM from Ferrier–Aligo microphysics and provides mass mixing ratios and particle sizes of individual hydrometeor species as input to the Community Radiative Transfer Model (CRTM; Han *et al.*, 2006), which is used by GSI to compute top-of-the-atmosphere radiances for a given HWRF background.

The first step of P6 formula uses F_ICE to determine the solid and liquid phases of CWM, that is,

$$\text{the solid phase of CWM} = \text{F\_ICE} \cdot \text{CWM} \tag{3}$$

and

$$\text{the liquid phase of CWM} = (1 - \text{F\_ICE}) \cdot \text{CWM} \tag{4}$$

Then, F_RAIN is used to partition the liquid phase of CWM into q_l and q_r as

$$q_l = (1 - \text{F\_RAIN}) \cdot (1 - \text{F\_ICE}) \cdot \text{CWM} \tag{5}$$

and

$$q_r = \text{F\_RAIN} \cdot (1 - \text{F\_ICE}) \cdot \text{CWM} \tag{6}$$

Similarly, the solid phase of CWM is decomposed into q_i and *precip_ice* as

$$q_i = w \cdot \text{F\_ICE} \cdot \text{CWM} \tag{7}$$

and

$$precip\_ice = (1 - w) \cdot \text{F\_ICE} \cdot \text{CWM} \tag{8}$$

where *precip_ice* is precipitating ice as opposed to q_i being the nonprecipitating ice, using an empirical weighting coefficient w

$$w = \begin{cases} 0.05 \cdot \frac{T - T_2}{T_1 - T_2} + 0.1 \cdot \frac{T - T_1}{T_2 - T_1} & \text{if} \quad T \le T_1 \\ 0.05 & \text{if} \quad T > T_1 \end{cases} \tag{9}$$

where T is temperature, $T_1 = 243.15$ K, and $T_2 = 233.15$ K.

Finally, depending on the values of F_RIMEF, *precip_ice* will be equal to either q_s, q_g, or q_h as follows

$$precip\_ice = \begin{cases} q_s & \text{if} \quad 1 \le \text{F\_RIMEF} \le 5 \\ q_g & \text{if} \quad 5 < \text{F\_RIMEF} \le 20 \\ q_h & \text{if} \quad \text{F\_RIMEF} > 20 \end{cases} \tag{10}$$

After the partition, individual hydrometeor species (q_l, q_i, q_r, q_s, q_g, and q_h) are used by the new observation operators, which are discussed next.

2.3. New observation operators

The new observation operator for integrated SWC, referred to as h_s, is defined as a vertical integration of the solid hydrometeor species including cloud ice, snow, graupel, and hail, that is,

$$h_s = \sum_{k=k_0}^{k_{\max}} \left(q_i^k + q_s^k + q_g^k + q_h^k \right) \cdot \frac{\Delta P^k}{g} \tag{11}$$

Similarly, the new observation operator for integrated LWC, referred to as h_l, is defined as a vertical integration of the liquid hydrometeor species including cloud water and rain, that is,

$$h_l = \sum_{k=1}^{k_{\text{mix}}} \left(q_l^k + q_r^k \right) \cdot \frac{\Delta P^k}{g} \tag{12}$$

A horizontal smoothing procedure is carried out prior to the vertical integration in Equations (11) and (12). This horizontal smoothing is done by applying a

formulation of recursive filter (Hayden and Purser, 1995) to the individual hydrometeor species. Such smoothing procedure was necessary because values of integrated SWC and integrated LWC computed by h_s and h_l from a given HWRF background were found much larger compared to observations during the preliminary development. As a result, large values of innovation were created and observations were rejected. The horizontal smoothing was used to reduce large innovations by smoothing individual hydrometeor fields. Reasons causing the large innovation values are left for future investigation, because they may be related to the cloud microphysics scheme and the P6 formula. In addition, the spatial resolution of Hurricane GPROF retrievals (5–10 km) is incomparable to the HWRF grid that has a grid spacing of 2 km. Due to the different resolutions, fine features that are associated with clouds and precipitations, which may be inferred from an HWRF background, may not be detected in the retrievals due to a coarse footprint size.

3. Experiments

Hurricane Gonzalo (2014) is used in this study. In order to have a large portion of Gonzalo covered by Hurricane GPROF data, only three analysis times are selected and they are (1) 0600 UTC 13 October, (2) 1200 UTC 16 October, and (3) 0600 UTC 17 October. Examples of integrated SWC and integrated LWC valid at these three times in the innermost domain of HWRF are displayed in Figure 1. In Figures 1(a) and (b), a less organized precipitation structure with no indication of the center of Gonzalo is seen in analysis time (1). In contrast, a well-defined spiral feature in Figures 1(c)–(f) is evident in both analysis times (2) and (3), which is indicative a mature hurricane.

3.1. Prepare for assimilation

Currently, HWRF only assimilates radiances under clear-sky condition. Therefore, there is no preparation of microphysical variables for a background field. Prior to data assimilation, vortex initialization is carried out to improve the HWRF hurricane vortex through a series of adjustments. After vortex initialization, a background field that contains an improved vortex is then provided and used by GSI. However, currently, adjustment of cloud microphysical variables was not considered by vortex initialization, hence, values of CWM and partition parameters are set to zero. In order to include cloud condensate variables in HWRF assimilation, techniques are developed in HWRF, which can be summarized in three procedures: (1) reinitialize CWM and F_ICE, F_RAIN, and F_RIMEF in the background prior to data assimilation, (2) add CWM as control variable and add individual hydrometeor species as state variables, and (3) include tangent linear and adjoint parts of P6 formula (Equations (3)–(10)) in the minimization of the cost function.

Specifically, in (1), a possible solution to avoid the zero-cloud-condensate situation was proposed. That is, values of CWM, F_ICE, F_RAIN, and F_RIMEF in the 6-h HWRF forecast from a previous HWRF cycle are mapped onto a background (same grid spacing) provided by vortex initialization. Since the center of a hurricane in the 6-h HWRF forecast may be different from the center of the observed one, three-dimensional fields of CWM and partition parameters from the 6-h HWRF forecast are horizontally shifted to the true center before mapping to the background. In (2), the cross-variable correlations between CWM and other variables are described by the hybrid background error covariance, in which 20% comes from a static component embedded in GSI (Wu *et al.*, 2002) and 80% comes from an ensemble component. For the static component that is based on the National Meteorological Center (NMC), the former name of National Centers for Environmental Prediction (NCEP) method (Parrish and Derber, 1992), the same correlations for q_v are used to describe the correlations for CWM. For the ensemble component, the 80-member GFS ensemble forecasts are used. Since Ferrier–Aligo microphysics scheme is employed by both GFS and HWRF, CWM is also a prognostic variable to GFS. By adding CWM as an additional control variable, correlations between CWM and other control variables estimated by both static and ensemble components will be included in the hybrid background error covariance. Consequently, the resulting analysis will contain a consistent update of CWM and other control variables. This is important as pointed out by Huang (1996) that a consistent treatment of cloud and other control variables can avoid imbalanced initial condition. In (3), by including tangent linear and adjoint parts of Equations (3)–(6) in the cost function minimization, conversions between individual hydrometeor state variables and CWM control variable are carried out during each iteration.

As mentioned above, the 80-member GFS ensemble is used by HWRF. There exists a potential undesirable impact on the HWRF analysis and forecast when non-native ensemble is used (e.g. vortex spindown as discussed by Pu *et al.*, 2016). Due to the different scales and architectures of the two models, background error covariance estimated by the GFS ensemble may be unable to accurately describe the cross-variable correlations of HWRF.

3.2. Experimental design

Two experiments are conducted that use two different pairs of observation operators and they are (1) CTL, which uses the 2015 HWRF operational configuration (Tallapragada *et al.*, 2015) and assimilates integrated SWC and integrated LWC retrievals using $h_{s\_noHydro}$ and $h_{l\_noHydro}$ while conventional observations are also assimilated in the innermost domain of HWRF, and (2) USEP6, the same as CTL, except that h_s and h_l are used instead. Both CTL and USEP6 experiments are conducted for Hurricane Gonzalo (2014) at the three analysis times.

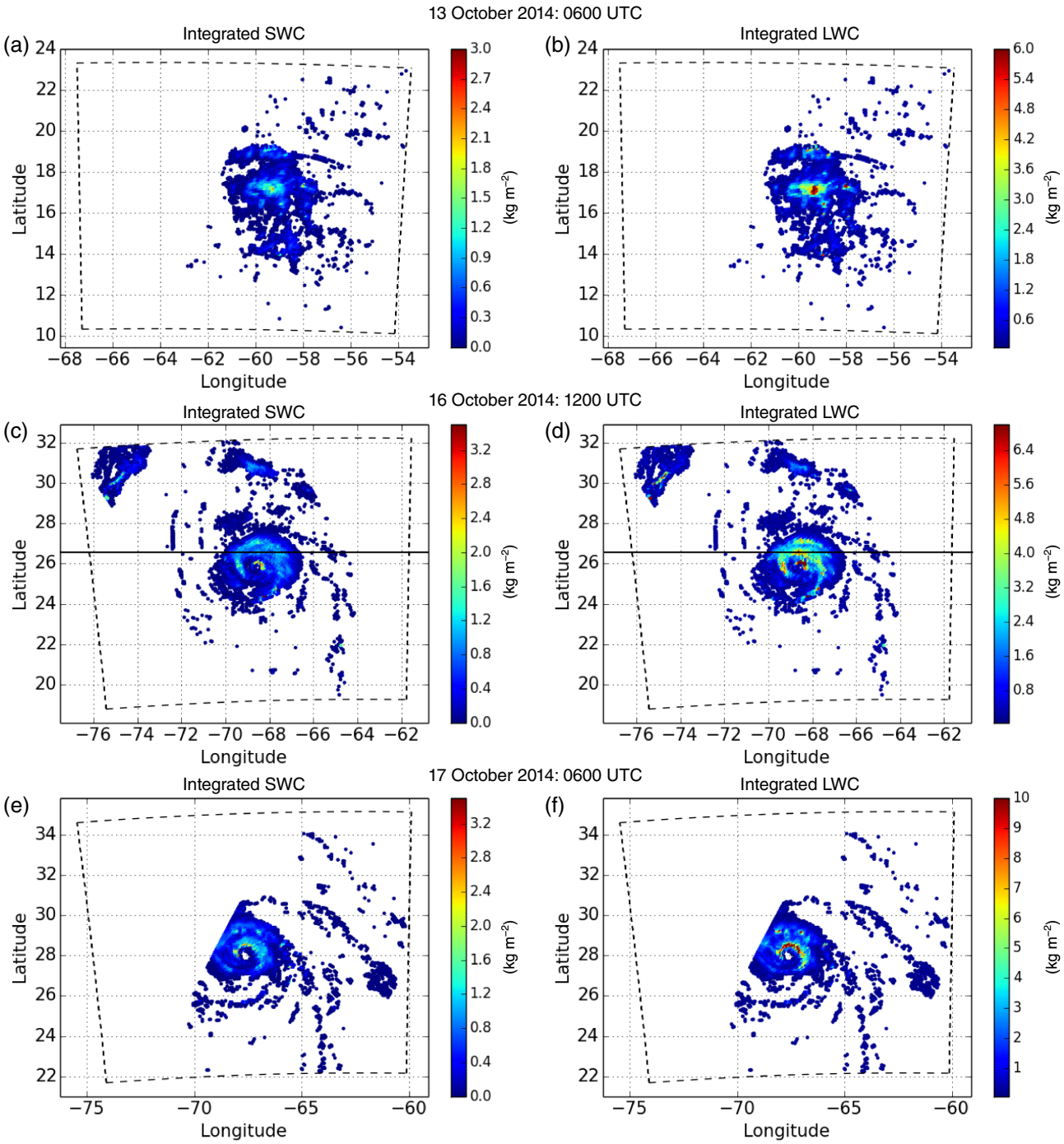

Figure 1. Hurricane GPROF retrieved (a) integrated SWC (kg m^{-2}) and (b) integrated LWC (kg m^{-2}) at 0600 UTC 13 October during Hurricane Gonzalo (2014). (c), (d) and (e), (f) are the same as (a) and (b), except that they are valid at 1200 UTC 16 October and 0600 UTC 17 October. A horizontal black line along 26.5°N in (c) and (d) indicates the latitude at which the cross-sections shown in Figure 3 were taken.

4. Results

4.1. Observed versus simulated

A scatterplot is produced to summarize the assimilation statistics from the three pairs of CTL (dots) and USEP6 (triangles) experiments. In Figure 2, statistics are presented in terms of the absolute values of background innovation (observation minus background), $|O-B|$, plotted on the y-axis and the absolute values of analysis innovation (observation minus analysis), $|O-A|$, plotted on the x-axis. A diagonal solid line will be referred to as the 1-1 line.

In general, there are more data points from USEP6 located above the 1-1 line. In Figure 2, 42% (45%) of the data points of integrated SWC (integrated LWC) from the CTL experiment (circles) are above the 1-1 line, while 55% (77%) of the data points of integrated SWC (integrated LWC) from the USEP6 experiment are above the 1-1 line. One may also notice that there exhibits a wider spread of USEP6 data points, which

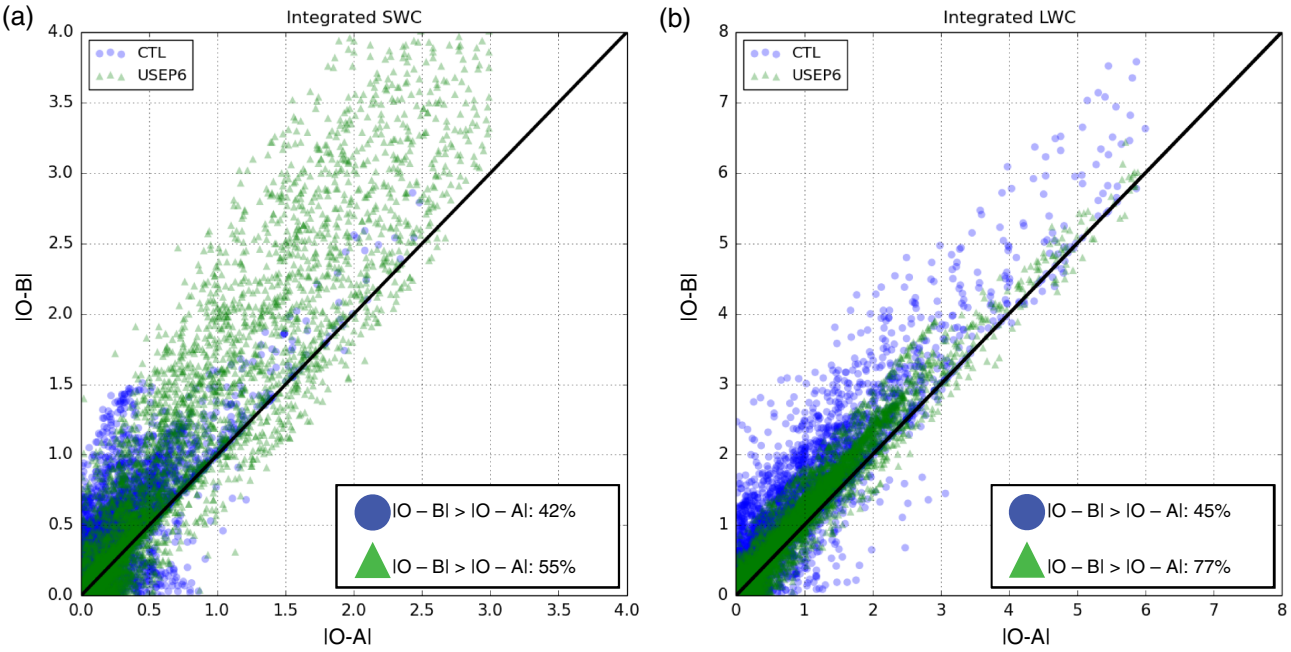

Figure 2. Scatterplot of absolute values of observation minus analysis ($|O - A|$) versus absolute values of observation minus background ($|O - B|$) from the three pairs of CTL (blue dots) and USEP6 (green triangle) experiments.

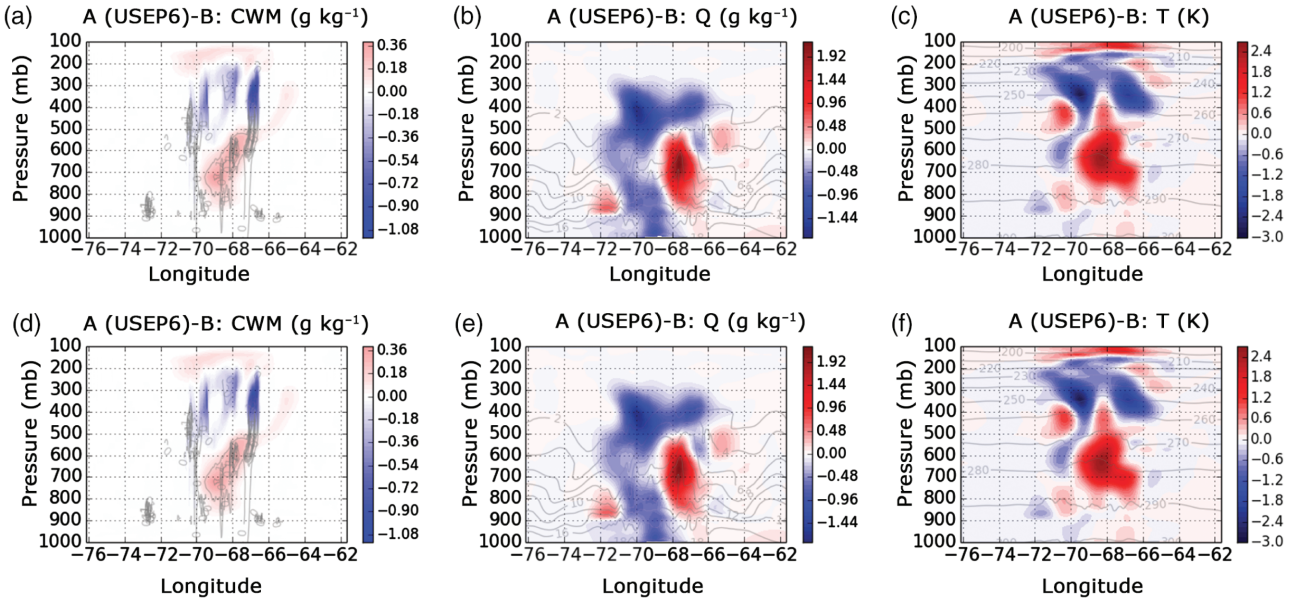

Figure 3. East–west cross-section of analysis increments (color) overlapped with background field (contour) from the USEP6 experiment: (a) CWM ($g\,kg^{-1}$), (b) specific humidity ($g\,kg^{-1}$), and (c) temperature (K). (d)–(f) are the same as (a)–(c), except for analysis increments from the CTL experiment.

suggest that there are many larger values of background innovation of integrated SWC produced when using h_s. In contrast, a narrower spread of USEP6 data points are seen in Figure 2(b) when using h_l is used. Nevertheless, USEP6 analysis was an improvement of fit to observations over the background (i.e. $|O-A| < |O-B|$) when compared to that of CTL, which is encouraging.

4.2. Analysis increments

A vertical cross-section of analysis increments (analysis minus background) for CWM, specific humidity, and temperature is produced. In Figure 3, analysis increments from both CTL and USEP6 experiments valid at 1200 UTC 16 October is displayed along 26.5°N (Figures 1(c) and (d)).

Nonzero CWM increments in the USEP6 experiments are evident in the region where observations are located (Figure 3(a)), while no CWM increments are displayed in CTL experiment (Figure 3(d)), as expected. Focusing on the USEP6 experiment, the increase of condensate between 600 and 900 hPa may be related to the liquid component of CWM, while the reduction between 200 and 500 hPa is likely due to the solid

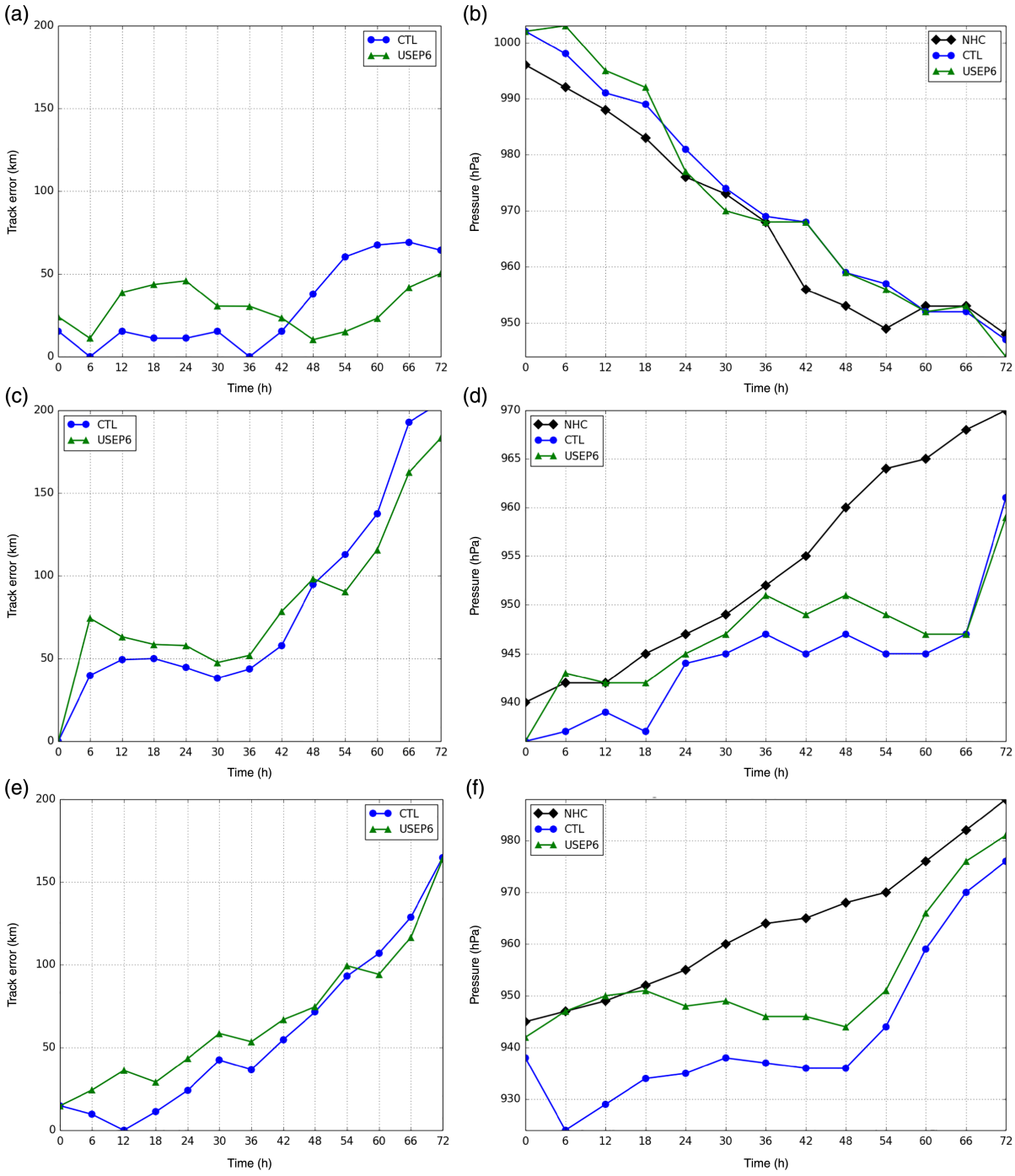

Figure 4. (a) Track error (km) and (b) MSLP (hPa) from the 72 h HWRF forecasts initialized using the CTL (blue) and USEP6 (green) analyses valid at 0600 UTC 13 October during Hurricane Gonzalo (2014). (c)–(d) and (e)–(f) are the same as (a)–(b), except for forecasts initialized at 1200 UTC 16 October and 0600 UTC 17 October, respectively. Black solid lines represent the corresponding estimates from NHC best-track data.

component (Figure 3(a)). These responses in CWM appear to coincide with the corresponding increments in specific humidity and temperature where warming and moistening is evident in lower troposphere and cooling and drying is more pronounced in upper troposphere (Figures 3(b) and (c)). On the other hand, the adjustments of specific humidity and temperature in the CTL experiment (Figures 3(e) and (f)) show a tendency to reach super-saturation by moistening and cooling the air column. Such adjustments are considerably different from the USEP6 experiment with additional constraints from CWM.

4.3. Hurricane track and intensity forecasts

Three pairs of 72-h HWRF forecasts initialized with CTL and USEP6 analyses are conducted. Forecast track error and intensity (minimum sea-level pressure; MSLP) from CTL and USEP6 are compared with best-track data from National Hurricane Center (NHC). Results suggest that USEP6 forecasts have slightly

larger track errors during the first 48 h, but the errors become smaller compared to CTL forecasts in the last 24 h (Figures 4(a), (c) and (e)). In general, the differences between the track errors from CTL and USEP6 forecasts are small. The intensity forecast as measured by MSLP from USEP6 is found closer to the NHC best-track values than CTL for the two forecasts initialized at 1200 UTC 16 October and 0600 UTC 17 October (Figures 4(d) and (f)). There is no obvious difference between the intensity forecasts initialized by CTL and USEP6 analyses valid at 0600 UTC 13 October when Gonzalo was a tropical storm (Figure 4(b)).

5. Summary and discussion

New observation operators are developed to extend upon the work by Wu *et al.* (2016). Due to the limitations that include a potential negative bias and the lack of cloud condensate updates from using observation operators based on super-saturation ($h_{\text{s\_noHydro}}$ and $h_{\text{l\_noHydro}}$), new observation operators are developed by directly using hydrometeor species estimated from cloud microphysical variables. Since the Ferrier–Aligo microphysics scheme predicts CWM rather than the individual hydrometeors, an empirical formula embedded in GSI is used to partition CWM into individual hydrometeor species. Then, the new observation operators, h_{s} and h_{l}, are defined as a vertical integration of solid and liquid hydrometeor species, respectively.

Hurricane Gonzalo (2014) is selected to perform three pairs of CTL and USEP6 experiments to examine the impact of assimilating retrieved integrated SWC and integrated LWC using $h_{\text{s\_noHydro}}$ and $h_{\text{l\_noHydro}}$ (CTL) and h_{s} and h_{l} (USEP6) on HWRF analysis and subsequent forecast. For USEP6 experiments, encouraging results are obtained, in which the analysis was an improvement of fit to observations over the background, when compared to CTL. Including CWM as a control variable is found to have a clear impact on other variables, such as specific humidity and temperature. In general, USEP6 experiment appears to result in similar forecast track to that of the CTL experiment. Nevertheless, the MSLP forecast from the USEP6 experiment shows some improvement over the CTL forecast in two of the three cases.

As stated earlier, cloud microphysics scheme is essential to the development of the new observation operators, h_{s} and h_{l}. As an operational model, HWRF is currently restricted to use a rather simple but computationally efficient scheme that predicts total cloud condensate instead of individual hydrometeor species. If switched to a more sophisticated microphysics scheme that predicts individual hydrometeor species, the partition formula may be avoided. As a result, individual hydrometeors are more accurately accounted for during data assimilation, thus, improved assimilation of the retrieved integrated SWC and integrated LWC is anticipated. In addition, the resulting analysis may be further improved by using the HWRF-based ensemble, which is a more optimal choice over the GFS ensemble.

Acknowledgements

This research is primarily funded by NOAA's Sandy Supplemental Award Number NA14OAR4830122. The assimilation experiments were performed using the Joint Center for Satellite Data Assimilation 'S4' supercomputer located at the University of Wisconsin-Madison. The authors would like to thank Drs. Krishna Kumar and Samuel Trahan for their help on porting the HWRF system onto S4. Encouraging discussions with Drs. Lewis Grasso and Paula Brown are greatly appreciated. The authors are also grateful to the two anonymous reviewers for their careful reviews and valuable comments.

References

Aligo E, Ferrier BS, Carley J, Rogers E, Pyle M, Weiss SJ, Jirak IL. 2014. Modified microphysics for use in high resolution NAM forecast. In 27th AMS Conference on Severe Local Storms, Madison, WI, 3–7 November 2014. https://ams.confex.com/ams/27SLS/webprogram/Paper255732.html (accessed 8 April 2017).

Bauer P, Geer AJ, Lopez P, Salmond D. 2010. Direct 4D-Var assimilation of all-sky radiances. Part I: Implementation. *Quarterly Journal of the Royal Meteorological Society* **136**: 1868–1885. https://doi.org/10.1002/qj.659.

Bauer P, Ohring G, Kummerow C, Auligne T. 2011. Assimilating satellite observations of clouds and precipitation into NWP models. *Bulletin of the American Meteorological Society* **92**: 25–28. https://doi.org/10.1175/2011BAMS3182.1.

Boukabara S-A, Garrett K, Grassotti C, Iturbide-Sanchez F, Chen W, Jiang Z, Clough SA, Zhan X, Liang P, Liu Q, Islam T, Zubko V, Mims A. 2013. A physical approach for a simultaneous retrieval of sounding, surface, hydrometeor, and cryospheric parameters from SNPP/ATMS. *Journal of Geophysical Research: Atmospheres* **118**: 12600–12619. https://doi.org/10.1002/2013JD020448.

Brown PJ, Kummerow CD, Randel DL. 2016. Hurricane GPROF: an optimized ocean microwave rainfall retrieval for tropical cyclones. *Journal of Atmospheric and Oceanic Technology* **33**: 1539–1556. https://doi.org/10.1175/JTECH-D-15-0234.1.

Han Y, van Delst P, Liu Q, Weng F, Yan B, Treadon R, Derber J. 2006. *JCSDA Community Radiative Transfer Model (CRTM) – version 1*. NOAA Technical Report NESDIS 122; 40 pp.

Hayden CM, Purser RJ. 1995. Recursive filter objective analysis of meteorological fields: applications to NESDIS operational processing. *Journal of Applied Meteorology* **34**: 3–15. https://doi.org/10.1175/1520-0450-34.1.3.

Huang XY. 1996. Initialization of cloud water content in a data assimilation system. *Monthly Weather Review* **124**: 478–486.

Kleist DT, Parrish DF, Derber JC, Treadon R, Wu W-S, Lord S. 2009. Introduction of the GSI into the NCEP global data assimilation system. *Weather and Forecasting* **24**: 1691–1705. https://doi.org/10.1175/2009WAF2222201.1.

Kummerow CD, Randel DL, Kulie M, Wang NY, Ferraro R, Joseph Munchak S, Petkovic V. 2015. The evolution of the Goddard profiling algorithm to a fully parametric scheme. *Journal of Atmospheric and Oceanic Technology* **32**: 2265–2280. https://doi.org/10.1175/JTECH-D-15-0039.1.

Parrish DF, Derber JC. 1992. The national meteorological center's spectral statistical-interpolation analysis system. *Monthly Weather Review* **120**: 1747–1763. https://doi.org/10.1175/1520-0493(1992)120<1747:TNMCSS>2.0.CO;2.

Pu Z, Zhang S, Tong M, Tallapragada V. 2016. Influence of the self-consistent regional ensemble background error covariance on hurricane inner-core data assimilation with the GSI-based hybrid system for HWRF. *Journal of the Atmospheric Sciences* **73**: 4911–4925. https://doi.org/10.1175/JAS-D-16-0017.1.

Tallapragada V, Bernadet L, Biswas MK, Ginis I, Kwon Y, Liu Q, Marchok T, Sheinin D, Thomas B, Tong M, Trahan S, Wang W, Yablonsky R, Zhang X. 2015. *Hurricane Weather Research and Forecasting (HWRF) Model: 2015 Scientific Documentation*. Developmental Testbed Center: Boulder, CO; 113.

Wang X. 2010. Incorporating ensemble covariance in the gridpoint statistical interpolation variational minimization: a mathematical framework. *Monthly Weather Review* **138**: 2990–2995. https://doi.org/10.1175/2010MWR3245.1.

Wu W-S, Purser RJ, Parrish DF. 2002. Three-dimensional variational analysis with spatially inhomogeneous covariances. *Monthly Weather Review* **130**: 2905–2916. https://doi.org/10.1175/1520-0493(2002)130<2905:TDVAWS>2.0.CO;2.

Wu T-C, Zupanski M, Grasso LD, Brown PJ, Kummerow CD, Knaff JA. 2016. The GSI capability to assimilate TRMM and GPM hydrometeor retrievals in HWRF. *Quarterly Journal of the Royal Meteorological Society* **142**: 2768–2787. https://doi.org/10.1002/qj.2867.

Zhu Y, Liu E, Mahajan R, Thomas C, Groff D, Van Delst P, Collard A, Kleist D, Treadon R, Derber JC. 2016. All-sky microwave radiance assimilation in NCEP's GSI analysis system. *Monthly Weather Review* **144**: 4709–4735. https://doi.org/10.1175/MWR-D-15-0445.1.